

# Few-body spin couplings and their implications for universal quantum computation

Ryan Woodworth<sup>1</sup>, Ari Mizel<sup>1,2</sup> and Daniel A Lidar<sup>3,4</sup>

<sup>1</sup> Physics Department, Pennsylvania State University, University Park, PA 16802, USA

<sup>2</sup> Materials Research Institute, Pennsylvania State University, University Park, PA 16802, USA

<sup>3</sup> Chemical Physics Theory Group, and Center for Quantum Information and Quantum Control, University of Toronto, 80 St George Street, Toronto, ON, M5S 3H6, Canada

<sup>4</sup> Departments of Chemistry and Electrical Engineering-Systems, University of Southern California, Los Angeles, CA 90089, USA

E-mail: [lidar@usc.edu](mailto:lidar@usc.edu)

Received 5 August 2005, in final form 7 September 2005

Published 12 May 2006

Online at [stacks.iop.org/JPhysCM/18/S721](http://stacks.iop.org/JPhysCM/18/S721)

## Abstract

Electron spins in semiconductor quantum dots are promising candidates for the experimental realization of solid-state qubits. We analyse the dynamics of a system of three qubits arranged in a linear geometry and a system of four qubits arranged in a square geometry. Calculations are performed for several quantum dot confining potentials. In the three-qubit case, three-body effects are identified that have an important quantitative influence upon quantum computation. In the four-qubit case, the full Hamiltonian is found to include both three-body and four-body interactions that significantly influence the dynamics in physically relevant parameter regimes. We consider the implications of these results for the encoded universality paradigm applied to the four-electron qubit code; in particular, we consider what is required to circumvent the four-body effects in an encoded system (four spins per encoded qubit) by the appropriate tuning of experimental parameters.

(Some figures in this article are in colour only in the electronic version)

## 1. Introduction

Electron spins in semiconductor quantum dots are a leading candidate for the physical realization of qubits in a quantum computer [1]. Although any quantum algorithm may be implemented using single-qubit and two-qubit gates [2], many such algorithms realize substantial increases in efficiency by exploiting simultaneous interactions among three or more qubits [3–16]. In order to employ such simultaneous interactions it is essential to understand in detail the many-body dynamics of the system of coupled qubits. More generally, since a

practical quantum computer may need to contain as many as  $10^6$  qubits [3] it is essential to characterize the effect of many-body interactions on the system's overall energy landscape.

In past work [17, 18], we used a model confining potential of superposed parabolic minima to demonstrate that three-body effects significantly influence the Hamiltonian of three electrons confined to three quantum dots at the vertices of an equilateral triangle and that four-body effects are significant for four electrons confined to a tetrahedral arrangement of four dots. (The introduction of a third spin adds no new terms to the Hamiltonian, but the coupling strength for each pair of spins is changed nontrivially by the presence of the third.) Here we extend these results in two ways. First, we analyse three quantum dots in a linear geometry [19] and four dots in a square geometry [20] since these geometries are more likely to occur in a real quantum computer apparatus. Second, by employing a Gaussian shape for the confining potential of each well [21] we explore the sensitivity of the many-body effects to the form of the confining potential. In both cases a non-perturbative calculation finds that many-body effects contribute appreciably to the Hamiltonian. We note that Scarola *et al* [22, 23] have demonstrated that the application of a magnetic field allows chiral terms to arise in the spin Hamiltonian, which modifies this Hamiltonian in another important manner as compared to the naïve Heisenberg form.

Hitherto, discussions of quantum dot quantum computation have nearly always assumed pairwise Heisenberg interactions. In view of the above result, this implies that computational errors may occur in the context of quantum computers using electron spin qubits in quantum dots, unless one always simultaneously couples only disjoint pairs of dots. There are at least four circumstances where this may be undesirable or even infeasible. One is fault tolerant quantum error correction, where simultaneous operations on several coupled dots have been associated with better error thresholds. A second is adiabatic quantum computation [11], in which the final Hamiltonian may include the simultaneous interactions that we discuss here. We will not analyse these possibilities here, although we believe that the methods we discuss below are relevant to them.

We will focus on two other contexts, that of 'encoded universality' (EU) [5–9] and that of computation on decoherence-free subspaces (DFSs) [5, 6, 24] and supercoherent qubits [10]. In these cases, the goal is to perform universal quantum computation using (in the case of EU) only the most easily controllable interaction or (in the case of DFS and supercoherence) using only interactions that preserve the code subspace, since that subspace offers protection against certain types of decoherence. (Strong and fast exchange interaction pulses can further be used to suppress decoherence [25] and to eliminate decoherence-induced leakage [26].)

We will refer to these cases collectively as 'encoded quantum computation'. It turns out that universal quantum computation using only the Heisenberg exchange interaction is an extremely attractive possibility in encoded models, and we will consider it in detail below. After establishing that four-body interaction terms can arise in a Heisenberg exchange Hamiltonian, we investigate the question of neutralizing their effect by using encoded qubits [5, 6, 8–10, 24–29]. By generalizing the work of Bacon [30], who showed that universal quantum computation was possible using encoded gates with two-body coupling Hamiltonians (i.e. assuming that the Heisenberg Hamiltonian was applicable even when coupling three or more dots at a time), we enumerate tuning conditions on experimental parameters that are needed for the four-body effects to cancel out. An alternative is to design these encoded gates while allowing only pairs of electrons to couple at any given time. This is indeed possible, as shown in [31] for the price of significantly longer pulse sequences per given encoded gate. Nevertheless, in view of the findings reported here and in [22, 23], this price may be worth paying.

## 2. Three-electron case

A system of three electrons within a confining scalar potential  $V(\mathbf{r})$  obeys the Hamiltonian

$$H = \sum_{i=1}^3 \left[ \frac{\mathbf{p}_i^2}{2m} + V(\mathbf{r}_i) \right] + \sum_{i<j} \frac{e^2}{\kappa|\mathbf{r}_i - \mathbf{r}_j|} \quad (1)$$

$$\equiv \sum_{i=1}^3 h(\mathbf{r}_i) + \sum_{i<j} w(\mathbf{r}_i, \mathbf{r}_j) \quad (2)$$

in the absence of spin–orbit coupling and external magnetic fields. Although [17] succeeded in demonstrating significant three-body and four-body effects in systems containing three or more electrons, a confining potential with quadratic minima has certain other characteristics which are unlikely to describe an experimental arrangement; for example, it diverges at large distances from the origin, and the single adjustable parameter  $\omega_0$  forces us to specify very narrow minima whenever we want a high barrier between them. We therefore begin with the Gaussian form

$$V(\mathbf{r}) = -V_0[e^{-\alpha|\mathbf{r}-\mathbf{A}|^2} + e^{-\alpha|\mathbf{r}-\mathbf{B}|^2} + e^{-\alpha|\mathbf{r}-\mathbf{C}|^2}] \quad (3)$$

which has two tunable parameters. The three fixed points are collinear and separated by a distance  $2l$ :  $\mathbf{A} = (-2l, 0, 0)$ ,  $\mathbf{B} = (0, 0, 0)$  and  $\mathbf{C} = (2l, 0, 0)$ .

We assume a Heitler–London approximation [32], wherein excited orbital states and states with double occupation of any single dot are neglected (see [23] for a recent discussion of the validity of this approximation in the context of electron spin qubits). The system’s only degrees of freedom are therefore the spins of the confined electrons, leading to a total of  $2^3 = 8$  ‘computational’ basis states

$$|\Psi(s_A, s_B, s_C)\rangle = \sum_P \delta_P P[|A\rangle |B\rangle |C\rangle |s_A\rangle |s_B\rangle |s_C\rangle]. \quad (4)$$

In the above,  $\{|A\rangle\}$  are the three localized orbital ground states;  $|s_{\{A\}}\rangle$  denote the corresponding spin states;  $P$  is the set of all permutations of  $\{A, B, C\}$ ;  $\delta_P$  is 1 (–1) for even (odd) permutations. For instance, one of the eight (unnormalized) basis states is

$$\begin{aligned} |\Psi(\uparrow\uparrow\downarrow)\rangle &= |ABC\rangle|\uparrow\uparrow\downarrow\rangle - |ACB\rangle|\uparrow\downarrow\uparrow\rangle + |CAB\rangle|\downarrow\uparrow\uparrow\rangle - |CBA\rangle|\downarrow\uparrow\uparrow\rangle \\ &+ |BCA\rangle|\uparrow\downarrow\uparrow\rangle - |BAC\rangle|\uparrow\uparrow\downarrow\rangle. \end{aligned}$$

To characterize the localized orbital state  $\{|A\rangle\}$  for each dot, we expand (3) to quadratic order and solve the Schrödinger equation as though the other potential wells were absent:

$$\phi_A(\mathbf{r}) \equiv \langle \mathbf{r} | A \rangle \equiv \left( \frac{m\omega_0}{\pi\hbar} \right)^{3/4} \exp\left(-\frac{m\omega_0}{2\hbar}|\mathbf{r} - \mathbf{A}|^2\right). \quad (5)$$

Unless  $\alpha$  is small compared to  $l^{-2}$ , this is of course a much coarser approximation than it would be for purely quadratic minima, so we refine it by centring  $\phi_A(\mathbf{r})$  and  $\phi_C(\mathbf{r})$  at the points which minimize  $\langle A|h|A\rangle$  and  $\langle C|h|C\rangle$ . Because these orbitals overlap at least slightly for any finite  $\omega_0$ , the states (4) are not orthogonal.

We now define  $H_{\text{spin}}$  to be the matrix representation of  $H$  in the basis (4), and expand it in terms of tensor products of Pauli matrices:

$$H_{\text{spin}} = \sum_{i,j,k} c_{ijk} \sigma_i \otimes \sigma_j \otimes \sigma_k.$$

This expansion is always possible, since the set of  $n$ -fold tensor products of Pauli matrices constitutes a complete orthonormal basis for the linear vector space of all  $2^n \times 2^n$  matrices. Because we have written the basis (4) in the form  $|s_A\rangle|s_B\rangle|s_C\rangle$  these Pauli matrices can be

associated with spin operators on each of the three quantum dots. For example, we can write  $\sigma_1 \otimes \sigma_3 \otimes \sigma_0 = 2S_{A,x} \otimes 2S_{B,z} \otimes I \equiv 4S_{A,x} S_{B,z}$ , where the notation  $S_{W,i}$  means the Pauli operator  $\sigma_i$  applied to the electron in the quantum dot at  $\mathbf{W}$  and where  $I$  is the  $2 \times 2$  identity matrix. (We exclude  $\hbar$  from the definition of the matrices  $\sigma_i$ ; thus,  $c_{ijk}$  have the dimensions of energy.) In the case of an arbitrary  $8 \times 8$  matrix, 64 complex numbers would be required to specify  $c_{ijk}$  fully, but the operator (1) clearly has certain properties which constrain the values of the coefficients, such as hermiticity, reflection symmetry, rotation symmetry, inversion symmetry and invariance under permutation of the electrons' labels. Once these symmetries have been accounted for, the  $c_{ijk}$  may be characterized by just three real quantities:

$$H_{\text{spin}} = K_0 + K_2[AB](\mathbf{S}_A \cdot \mathbf{S}_B + \mathbf{S}_B \cdot \mathbf{S}_C) + K_2[AC]\mathbf{S}_A \cdot \mathbf{S}_C, \quad (6)$$

where  $\mathbf{S}_W \cdot \mathbf{S}_V = S_{W,x} S_{V,x} + S_{W,y} S_{V,y} + S_{W,z} S_{V,z}$  and  $K_2[ij]$  is the pairwise coupling coefficient between the spins of the electrons in dots  $i$  and  $j$ . Here and elsewhere, we use symmetry considerations to reduce the number of coupling coefficients in our equations; in this case, the reflection symmetry of (3) through the  $x$ - $z$  plane implies that  $K_2[AB] = K_2[BC]$ . Physically, the constant  $K_2[AB]$  quantifies the coupling between adjacent spins while  $K_2[AC]$  describes the coupling between the spins at opposite ends of the row.

Defining  $\mathbf{S}_T = \mathbf{S}_A + \mathbf{S}_B + \mathbf{S}_C$ , one finds that

$$H_{\text{spin}} = L_0 + L_1 \mathbf{S}_T^2 + L'_1 (\mathbf{S}_A + \mathbf{S}_C)^2 \quad (7)$$

where

$$\begin{aligned} K_0 &= L_0 + \frac{9}{4}L_1 + \frac{3}{2}L'_1 \\ K_2[AB] &= 2L_1 \\ K_2[AC] &= 2L_1 + 2L'_1. \end{aligned} \quad (8)$$

The expansion (7) reveals that any simultaneous eigenstate of  $(\mathbf{S}_A + \mathbf{S}_C)^2$  and  $\mathbf{S}_T^2$  is also an eigenstate of  $H_{\text{spin}}$ . We can construct such simultaneous eigenstates by using the Clebsch–Gordan table twice, first to combine the spin of the electron in dot  $A$  with the spin of the electron in dot  $C$ , and then to combine that spin-1 (or spin-0) system with the spin of the electron in dot  $B$ :

$$\begin{aligned} \left| \frac{3}{2}, \frac{3}{2}; 1 \right\rangle &= |\Psi(\uparrow\uparrow\uparrow)\rangle \\ \left| \frac{3}{2}, \frac{1}{2}; 1 \right\rangle &= |\Psi(\uparrow\uparrow\downarrow)\rangle + |\Psi(\uparrow\downarrow\uparrow)\rangle + |\Psi(\downarrow\uparrow\uparrow)\rangle \\ \left| \frac{3}{2}, -\frac{1}{2}; 1 \right\rangle &= |\Psi(\downarrow\downarrow\uparrow)\rangle + |\Psi(\downarrow\uparrow\downarrow)\rangle + |\Psi(\uparrow\downarrow\downarrow)\rangle \\ \left| \frac{3}{2}, -\frac{3}{2}; 1 \right\rangle &= |\Psi(\downarrow\downarrow\downarrow)\rangle \\ \left| \frac{1}{2}, \frac{1}{2}; 1 \right\rangle &= 2|\Psi(\uparrow\downarrow\uparrow)\rangle - |\Psi(\uparrow\uparrow\downarrow)\rangle - |\Psi(\downarrow\uparrow\uparrow)\rangle \\ \left| \frac{1}{2}, -\frac{1}{2}; 1 \right\rangle &= 2|\Psi(\downarrow\uparrow\downarrow)\rangle - |\Psi(\downarrow\downarrow\uparrow)\rangle - |\Psi(\uparrow\downarrow\downarrow)\rangle \\ \left| \frac{1}{2}, \frac{1}{2}; 0 \right\rangle &= |\Psi(\uparrow\uparrow\downarrow)\rangle - |\Psi(\downarrow\uparrow\uparrow)\rangle \\ \left| \frac{1}{2}, -\frac{1}{2}; 0 \right\rangle &= |\Psi(\downarrow\downarrow\uparrow)\rangle - |\Psi(\uparrow\downarrow\downarrow)\rangle, \end{aligned} \quad (9)$$

where the indices on the left-hand side denote the values of  $S_T$ ,  $S_{T,z}$  and  $|\mathbf{S}_A + \mathbf{S}_C|$  respectively. Although the states  $|\Psi(s_A, s_B, s_C)\rangle$  are not orthonormal, the eight states (9) are orthogonal, and they are also eigenvectors of the  $8 \times 8$  matrix (7), which means that  $H_{\text{spin}}$  has been diagonalized. To obtain the parameters  $\{L_0, L_1, L'_1\}$  we will choose three eigenstates with different good quantum numbers, and observe that their energies can be evaluated either by matrix algebra or by integrating microscopically over the axes  $\mathbf{r}_i$  and the spins to compute the expectation value of (1):

$$\langle \Psi | H_{\text{spin}} | \Psi \rangle = \langle \Psi | H | \Psi \rangle. \quad (10)$$

Inserting (7) into the left-hand side, for three distinct combinations of the good quantum numbers  $\{(\mathbf{S}_A + \mathbf{S}_C)^2, S_T^2\}$ , yields

$$\begin{aligned} \frac{\langle \frac{3}{2} \frac{3}{2}; 1 | H_{\text{spin}} | \frac{3}{2} \frac{3}{2}; 1 \rangle}{\langle \frac{3}{2} \frac{3}{2}; 1 | \frac{3}{2} \frac{3}{2}; 1 \rangle} &= L_0 + \frac{15}{4} L_1 + 2L'_1 \\ \frac{\langle \frac{1}{2} \frac{1}{2}; 1 | H_{\text{spin}} | \frac{1}{2} \frac{1}{2}; 1 \rangle}{\langle \frac{1}{2} \frac{1}{2}; 1 | \frac{1}{2} \frac{1}{2}; 1 \rangle} &= L_0 + \frac{3}{4} L_1 + 2L'_1 \\ \frac{\langle \frac{1}{2} \frac{1}{2}; 0 | H_{\text{spin}} | \frac{1}{2} \frac{1}{2}; 0 \rangle}{\langle \frac{1}{2} \frac{1}{2}; 0 | \frac{1}{2} \frac{1}{2}; 0 \rangle} &= L_0 + \frac{3}{4} L_1 \end{aligned} \quad (11)$$

while the corresponding wavefunctions (9) turn the right-hand side into

$$\begin{aligned} E_{\frac{3}{2}, \frac{3}{2}; 1} &= \frac{\langle \Psi(\uparrow\uparrow\uparrow) | H | \Psi(\uparrow\uparrow\uparrow) \rangle}{\langle \Psi(\uparrow\uparrow\uparrow) | \Psi(\uparrow\uparrow\uparrow) \rangle} \\ E_{\frac{1}{2}, \frac{1}{2}; 1} &= \frac{\langle \Psi(\uparrow\uparrow\downarrow) | H | \Psi(\uparrow\uparrow\downarrow) \rangle + 2\langle \Psi(\uparrow\downarrow\uparrow) | H | \Psi(\uparrow\downarrow\uparrow) \rangle - 4\langle \Psi(\uparrow\uparrow\downarrow) | H | \Psi(\uparrow\downarrow\uparrow) \rangle + \langle \Psi(\uparrow\uparrow\downarrow) | H | \Psi(\downarrow\uparrow\uparrow) \rangle}{\langle \Psi(\uparrow\uparrow\downarrow) | \Psi(\uparrow\uparrow\downarrow) \rangle + 2\langle \Psi(\uparrow\downarrow\uparrow) | \Psi(\uparrow\downarrow\uparrow) \rangle - 4\langle \Psi(\uparrow\uparrow\downarrow) | \Psi(\uparrow\downarrow\uparrow) \rangle + \langle \Psi(\uparrow\uparrow\downarrow) | \Psi(\downarrow\uparrow\uparrow) \rangle} \\ E_{\frac{1}{2}, \frac{1}{2}; 0} &= \frac{\langle \Psi(\uparrow\uparrow\downarrow) | H | \Psi(\uparrow\uparrow\downarrow) \rangle - \langle \Psi(\uparrow\uparrow\downarrow) | H | \Psi(\downarrow\uparrow\uparrow) \rangle}{\langle \Psi(\uparrow\uparrow\downarrow) | \Psi(\uparrow\uparrow\downarrow) \rangle - \langle \Psi(\uparrow\uparrow\downarrow) | \Psi(\downarrow\uparrow\uparrow) \rangle}. \end{aligned} \quad (12)$$

The evaluation of these matrix elements and overlap integrals is a tedious, but straightforward procedure given the microscopic forms of  $H$  and  $\psi(\mathbf{r})$  in (1), (3) and (5). Combining equations (8), (11) and (12), we thus compute  $K_0$ ,  $K_2[AB]$  and  $K_2[AC]$  in terms of  $\omega_0$  and the dimensionless system parameters

$$x_b \equiv \frac{\frac{1}{2} m \omega_0^2 l^2}{\frac{1}{2} \hbar \omega_0} = \frac{m \omega_0 l^2}{\hbar} \quad (13)$$

$$x_c \equiv \frac{e^2}{\kappa l \hbar \omega_0} \quad (14)$$

$$x_v \equiv \frac{2V_0}{\hbar \omega_0}. \quad (15)$$

Physically, the quantity  $x_b$  is the ratio of the height of the potential barrier between wells to the energy of the orbital ground state (5), while  $x_c$  is the ratio of the equilibrium Coulomb repulsion potential to the energy of the orbital ground state and  $x_v$  is the ratio of the individual well depth  $V_0$  to the ground state energy.

Here and in the following section, we have estimated experimentally relevant values of  $x_b$  and  $x_c$  as is done in [1]. We assume that the width of the function (5), which is  $2\sqrt{\hbar/m\omega_0}$ , must be roughly equal to the separation between adjacent dots  $2l$ ; using (13) we conclude that  $x_b \approx 1$ . For GaAs heterostructure single dots,  $\kappa \approx 13$ ,  $m^* \approx 0.067 m_e$  and  $\hbar\omega_0 \approx 3$  meV, which according to (14) means that  $x_c \approx 1.5$ .

A potential of the form (3) is most suitable for quantum computation when  $\alpha l^2$  is close to 1; if the inverted Gaussian decays too quickly in space, the spin coupling in the system becomes negligible, and if it decays too slowly, the local minima in  $V$  tend to coalesce at the centre. Using  $\frac{1}{2}\hbar\omega_0 \sim 1$  meV,  $V_0 \approx 3$  meV [1] and our prior estimate of  $x_c \approx 1.5$ , we obtain the relation  $x_b \approx x_v \sim 3$  by applying (13), (14) and (15). Noting that the parameter  $x_c$  has very little influence on any of the coupling constants over physically realistic ranges of  $x_b$  and  $x_v$  (and in any event depends on quantities, such as  $\kappa$ , which are difficult to tune experimentally) we henceforth set  $x_c = 1.5$ .

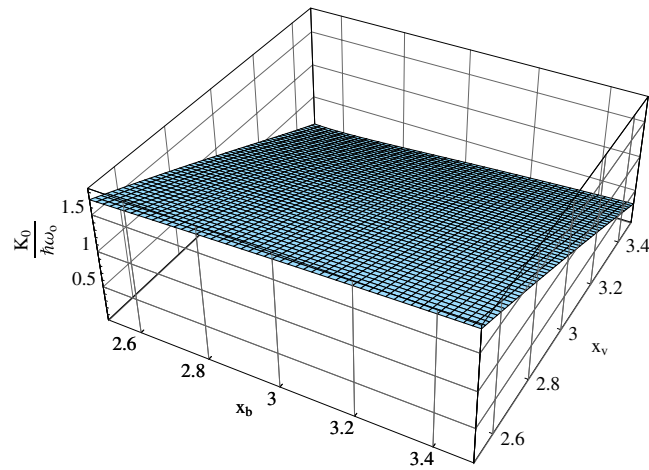


**Figure 1.** Plot of  $K_0$ , the overall energy shift, as a function of dimensionless barrier height  $x_b$  and overall well depth  $x_v$  in the case of three mutually interacting electrons in a linear geometry. In this and subsequent figures the Coulomb repulsion parameter  $x_c$  is set to 1.5 as in [17].

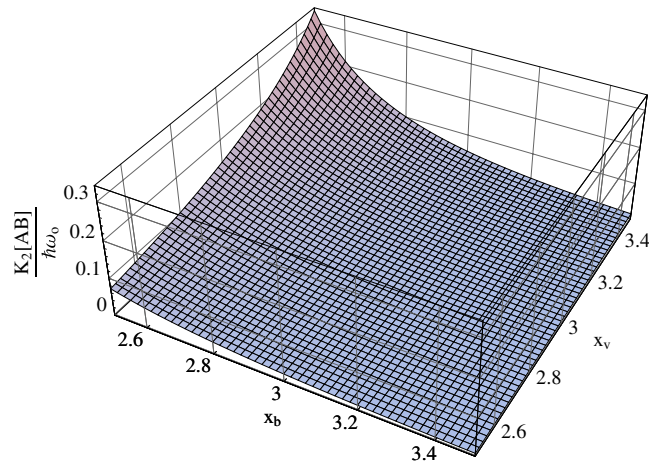


**Figure 2.** Plot of  $K_2[AB]$ , the two-body coupling coefficient for adjacent dots, as a function of dimensionless barrier height  $x_b$  and overall well depth  $x_v$  in the case of three mutually interacting electrons in a linear geometry.

Figure 1 shows the energy shift  $K_0$  as a function of the system parameters  $\{x_b, x_v\}$ . As one might expect, this spin-independent quantity increases with increasing  $x_v$  and decreasing  $x_b$  (whenever  $\omega_0$  decreases, there is greater orbital overlap and thus more Coulomb repulsion, irrespective of spin state). The coupling constants  $K_2[AB]$  and  $K_2[AC]$  are plotted in figures 2 and 3 respectively. We notice that they differ (which rules out the simple Heisenberg form  $H_{\text{spin}} = J \sum_{i < j} (\mathbf{S}_i \cdot \mathbf{S}_j)$ ), and that  $K_2[AC]$  is only about an order of magnitude smaller than  $K_2[AB]$  as we have confirmed by studying  $K_2[AB](x_b, x_v)$  and  $K_2[AC](x_b, x_v)$  on a logarithmic scale. In the context of quantum computation, this demonstrates that a nearest-neighbour approximation for the coupling between dots is insufficient (see also [23], where a similar conclusion was reported using a low-energy Hubbard model with one electron per site).

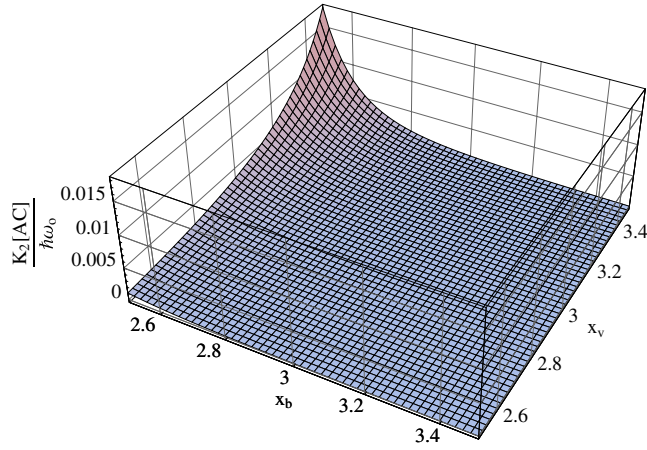


**Figure 3.** Plot of  $K_2[AC]$ , the two-body coupling coefficient for non-adjacent dots, as a function of dimensionless barrier height  $x_b$  and overall well depth  $x_v$  in the case of three mutually interacting electrons in a linear geometry.

### 3. Four-electron case

For the case of four quantum dots arranged in a square of side  $2l$  our formalism is more complex in detail but identical in structure. We therefore describe the computation only in outline.

The confining potential in the coordinate Hamiltonian

$$H = \sum_{i=1}^4 \left[ \frac{\mathbf{p}_i^2}{2m} + V(\mathbf{r}_i) \right] + \sum_{i<j} \frac{e^2}{\kappa |\mathbf{r}_i - \mathbf{r}_j|} \quad (16)$$

now becomes

$$V(\mathbf{r}) = -V_0 [e^{-\alpha|\mathbf{r}-\mathbf{A}|^2} + e^{-\alpha|\mathbf{r}-\mathbf{B}|^2} + e^{-\alpha|\mathbf{r}-\mathbf{C}|^2} + e^{-\alpha|\mathbf{r}-\mathbf{D}|^2}],$$

where  $\mathbf{A} = (0, 2l, 0)$ ,  $\mathbf{B} = (2l, 2l, 0)$ ,  $\mathbf{C} = (2l, 0, 0)$  and  $\mathbf{D} = (0, 0, 0)$ . Our computational basis consists of 16 fully antisymmetrized vectors of the form

$$|\Psi(s_A, s_B, s_C, s_D)\rangle = \sum_P \delta_P P[|A\rangle |B\rangle |C\rangle |D\rangle] \otimes |s_A\rangle |s_B\rangle |s_C\rangle |s_D\rangle. \quad (17)$$

The form of  $\phi(\mathbf{r})$  remains the same; to maintain the required geometrical symmetries, we now shift all four localized orbital wavefunctions an equal distance towards the point  $(l, l, 0)$ .

Expanding  $H$  in terms of products of Pauli matrices, as in

$$H_{\text{spin}} = \sum_{i,j,k,\ell} c_{ijkl} \sigma_i \otimes \sigma_j \otimes \sigma_k \otimes \sigma_\ell,$$

we discover by applying the symmetries of (16) that four-body terms now appear with nonzero coupling coefficients:

$$\begin{aligned} H_{\text{spin}} = & K_0 + K_2[AB](\mathbf{S}_A \cdot \mathbf{S}_B + \mathbf{S}_B \cdot \mathbf{S}_C + \mathbf{S}_C \cdot \mathbf{S}_D + \mathbf{S}_D \cdot \mathbf{S}_A) + K_2[AC](\mathbf{S}_A \cdot \mathbf{S}_C + \mathbf{S}_B \cdot \mathbf{S}_D) \\ & + K_4[ABCD][(\mathbf{S}_A \cdot \mathbf{S}_B)(\mathbf{S}_C \cdot \mathbf{S}_D) + (\mathbf{S}_B \cdot \mathbf{S}_C)(\mathbf{S}_D \cdot \mathbf{S}_A)] \\ & + K_4[ACBD](\mathbf{S}_A \cdot \mathbf{S}_C)(\mathbf{S}_B \cdot \mathbf{S}_D), \end{aligned} \quad (18)$$

where  $K_4[ijkl]$  is the four-body coupling coefficient among the spins of the electrons in dots  $i, j, k$  and  $\ell$ . Physically, the constant  $K_2[AB]$  describes the pairwise coupling between adjacent spins, while  $K_2[AC]$  describes the pairwise coupling between non-adjacent spins,

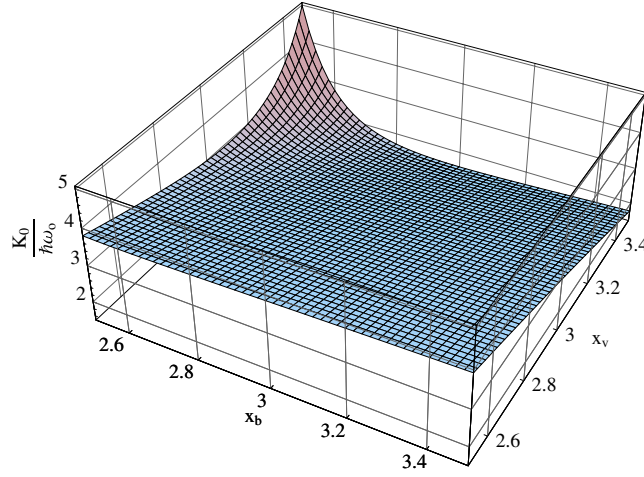


**Figure 4.** Plot of  $K_0$ , the overall energy shift, as a function of dimensionless barrier height  $x_b$  and overall well depth  $x_v$  in the case of four mutually interacting electrons in a square geometry.

$K_4[ABCD]$  describes four-body interactions concentrating on pairs of adjacent spins and  $K_4[ACBD]$  describes four-body interactions concentrating on pairs of non-adjacent spins. We define  $S_T = \mathbf{S}_A + \mathbf{S}_B + \mathbf{S}_C + \mathbf{S}_D$ , which leads us to

$$H_{\text{spin}} = L_0 + L_1 \mathbf{S}_T^2 + L'_1 [(\mathbf{S}_A + \mathbf{S}_C)^2 + (\mathbf{S}_B + \mathbf{S}_D)^2] + L_2 (\mathbf{S}_T^2)^2 + L'_2 (\mathbf{S}_A + \mathbf{S}_C)^2 (\mathbf{S}_B + \mathbf{S}_D)^2 \quad (19)$$

where

$$\begin{aligned} K_0 &= L_0 + 3L_1 + 3L'_1 + \frac{45}{2}L_2 + \frac{9}{4}L'_2 \\ K_2[AB] &= 2L_1 + 24L_2 \\ K_2[AC] &= 2L_1 + 2L'_1 + 24L_2 + 3L'_2 \\ K_4[ABCD] &= 8L_2 \\ K_4[ACBD] &= 8L_2 + 4L'_2. \end{aligned} \quad (20)$$

Applying the Clebsch–Gordan table three times creates 16 simultaneous eigenstates of  $(\mathbf{S}_A + \mathbf{S}_C)^2$ ,  $(\mathbf{S}_B + \mathbf{S}_D)^2$  and  $S_T^2$ . Inserting five of these states with different quantum numbers into (10) yields five equations for the five unknowns  $\{L_0, L_1, L'_1, L_2, L'_2\}$  in terms of the eigenstate energies. As before, these energies may be expressed in closed form as functions of  $x_b$ ,  $x_c$  and  $x_v$  by integrating the right-hand side of (10) explicitly.

The energy shift  $K_0$  for the square case is plotted in figure 4; as before, this constant is largest for strongly Coulomb-coupled dots separated by low potential barriers. Figures 5–8 depict the coupling coefficients  $K_2[AB]$ ,  $K_2[AC]$ ,  $K_4[ABCD]$  and  $K_4[ACBD]$  respectively. The departure from the pairwise Heisenberg picture is even more pronounced here: we see that for physically relevant values of the parameters  $\{x_b, x_v\}$  the four-body coefficient  $K_4[ACBD]$  is of the same order of magnitude as the two-body coefficient  $K_2[AC]$ , while  $K_4[ABCD]/K_2[AB] \sim 0.1$  as is confirmed by plotting  $K_2[AB](x_b, x_v)$ ,  $K_2[AC](x_b, x_v)$ ,  $K_4[ABCD](x_b, x_v)$  and  $K_4[ACBD](x_b, x_v)$  on a logarithmic scale. Typically  $K_4[ACBD]$  is opposite in sign to  $K_2[AC]$ , leading to a particularly important competition between the two-body and four-body interactions.

In order to confirm that the qualitative similarities between our final results and those of [17] were not artefacts of having made two broad changes to  $V(\mathbf{r})$  rather than one, we



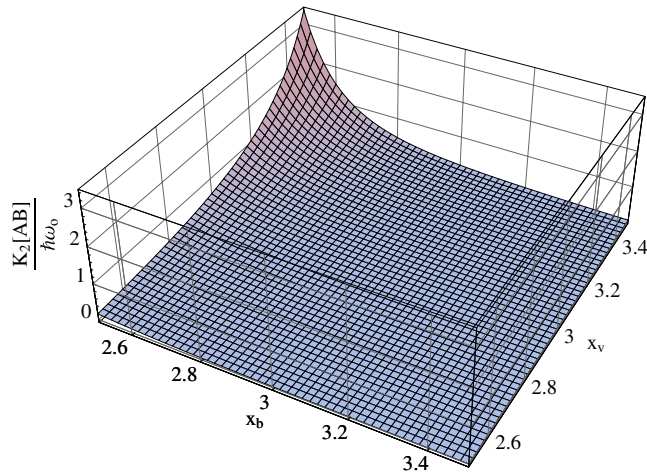


**Figure 5.** Plot of  $K_2[AB]$ , the two-body coupling coefficient for adjacent dots, as a function of dimensionless barrier height  $x_b$  and overall well depth  $x_v$  in the case of four mutually interacting electrons in a square geometry.

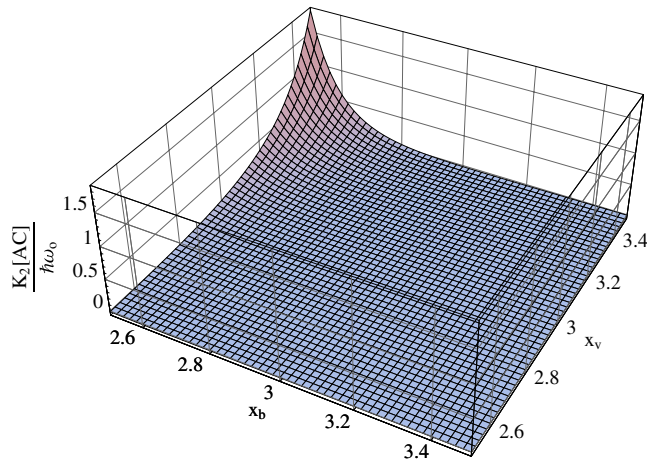


**Figure 6.** Plot of  $K_2[AC]$ , the two-body coupling coefficient for non-adjacent dots, as a function of dimensionless barrier height  $x_b$  and overall well depth  $x_v$  in the case of four mutually interacting electrons in a square geometry.

also analysed both the  $N = 3$  and 4 dot geometries using a confining potential of superposed quadratic minima. The variation of the coupling coefficients, within experimentally relevant ranges of  $x_b$  and  $x_c$  (analogous to figures 1 through 8), strongly resembled that for the Gaussian potential in all cases.

#### 4. Computing in the presence of four-body interactions using encoded qubits

We have shown that coupling three dots simultaneously quantitatively modifies the value of the exchange constant, and that coupling four dots simultaneously switches on a four-body interaction term of the form  $K_4[ABCD](S_A \cdot S_B)(S_C \cdot S_D)$  and its permutations. This

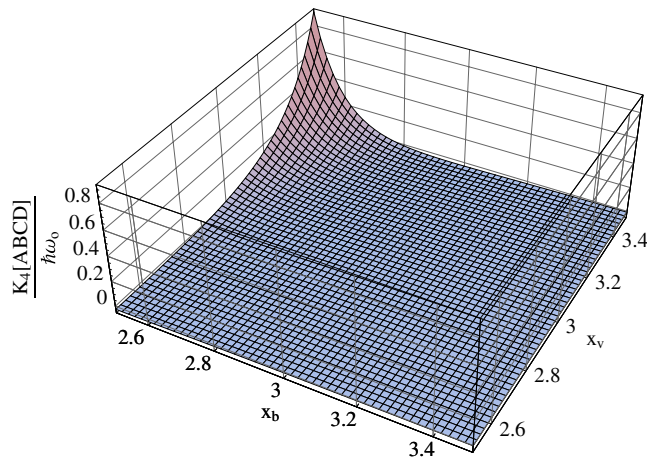


**Figure 7.** Plot of  $K_4[ABCD]$ , the four-body coupling coefficient for pairs of adjacent dots, as a function of dimensionless barrier height  $x_b$  and overall well depth  $x_v$  in the case of four mutually interacting electrons in a square geometry.

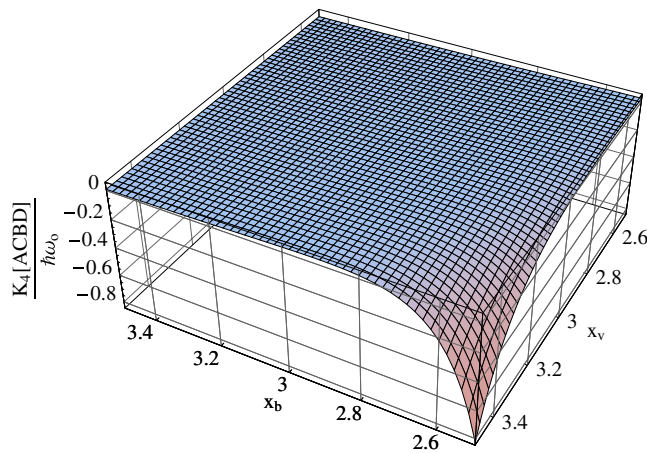


**Figure 8.** Plot of  $K_4[ACBD]$ , the four-body coupling coefficient for pairs of non-adjacent dots, as a function of dimensionless barrier height  $x_b$  and overall well depth  $x_v$  in the case of four mutually interacting electrons in a square geometry. Note that two of the axis directions are reversed from the preceding figures.

conclusion appears to be robust under changes in dot geometry and in the confining potential. A natural question is whether there exist methods to cancel the four-body correction. The issue is particularly urgent when one considers encoded quantum computation (EQC). In many known constructions of universal gates for EQC [5–10, 24–29, 31] there arises the need to simultaneously couple several spins. One of the most popular codes, described in detail below, uses four spins per encoded or logical qubit [5, 6, 8–10, 24–29]. For this code, universal computation requires that four spins be coupled at the same time using pairwise Heisenberg interactions. Hence *a priori* it appears that EQC using the four-qubit code suffers from a fundamental flaw. We now explore whether the four-qubit code may be implemented in such a way that each four-body coupling is either cancelled or reduced to an overall phase. Our

findings highlight problems that the four-body terms present in the context of EQC and also provide an interesting perspective on how the four-body terms may need to be dealt with in general.

#### 4.1. The code

Let us describe the four-spin DFS code, first proposed in [27] in the context of providing immunity against collective decoherence processes (see [29] for a review). Let the singlet and triplet states of two electrons  $i, j$  be denoted as

$$\begin{aligned} |s\rangle_{ij} &\equiv |S = 0, m_S = 0\rangle = \frac{1}{\sqrt{2}} (|\Psi(\uparrow\downarrow)\rangle - |\Psi(\downarrow\uparrow)\rangle) \\ |t_-\rangle_{ij} &\equiv |S = 1, m_S = -1\rangle = |\Psi(\downarrow\downarrow)\rangle \\ |t_0\rangle_{ij} &\equiv |S = 1, m_S = 0\rangle = \frac{1}{\sqrt{2}} (|\Psi(\uparrow\downarrow)\rangle + |\Psi(\downarrow\uparrow)\rangle) \\ |t_+\rangle_{ij} &\equiv |S = 1, m_S = 1\rangle = |\Psi(\uparrow\uparrow)\rangle. \end{aligned}$$

Then a single encoded DFS qubit is formed by the two singlets of four spins, i.e. the two states with zero total spin  $S_T = |\mathbf{S}_A + \mathbf{S}_B + \mathbf{S}_C + \mathbf{S}_D|$ . These states are formed by combining two singlets of two pairs of spins ( $|0_L\rangle$ ), or triplets of two pairs of spins ( $|1_L\rangle$ ), with appropriate Clebsch–Gordan coefficients:

$$\begin{aligned} |0_L\rangle &= |s\rangle_{AB} \otimes |s\rangle_{CD} = \frac{1}{2} (|\Psi(\uparrow\downarrow\uparrow\downarrow)\rangle + |\Psi(\downarrow\uparrow\downarrow\uparrow)\rangle \\ &\quad - |\Psi(\uparrow\downarrow\downarrow\uparrow)\rangle - |\Psi(\downarrow\uparrow\uparrow\downarrow)\rangle) \end{aligned} \quad (21)$$

$$\begin{aligned} |1_L\rangle &= \frac{1}{\sqrt{3}} (|t_-\rangle_{AB} \otimes |t_+\rangle_{CD} - |t_0\rangle_{AB} \otimes |t_0\rangle_{CD} + |t_+\rangle_{AB} \otimes |t_-\rangle_{CD}) \\ &= \frac{1}{\sqrt{3}} (2|\Psi(\uparrow\uparrow\downarrow\downarrow)\rangle + 2|\Psi(\downarrow\downarrow\uparrow\uparrow)\rangle - |\Psi(\uparrow\downarrow\downarrow\uparrow)\rangle \\ &\quad - |\Psi(\downarrow\uparrow\uparrow\downarrow)\rangle - |\Psi(\uparrow\downarrow\uparrow\downarrow)\rangle - |\Psi(\downarrow\uparrow\downarrow\uparrow)\rangle). \end{aligned} \quad (22)$$

As shown in [5, 6], the Heisenberg interaction  $\mathbf{S}_i \cdot \mathbf{S}_j$  can be used all by itself to implement universal quantum computation on this type of system. The Heisenberg interaction is closely related to the exchange operator  $E_{ij}$ , defined as

$$E_{ij} = \begin{pmatrix} 1 & & & \\ & 0 & 1 & \\ & 1 & 0 & \\ & & & 1 \end{pmatrix} \quad (23)$$

via  $E_{ij} = \frac{1}{2}(4\mathbf{S}_i \cdot \mathbf{S}_j + I)$ . The difference in their action as gates is only a phase; hence we will use  $E_{ij}$  and  $\mathbf{S}_i \cdot \mathbf{S}_j$  interchangeably from now on and write  $E_{ij} \simeq \mathbf{S}_i \cdot \mathbf{S}_j$ . The  $E_{ij}$  have a simple action on the electronic spin up/down states, as seen from the matrix representation (23): the states  $|00\rangle$  and  $|11\rangle$  are invariant whereas  $|01\rangle$  and  $|10\rangle$  are exchanged. Using this, it is simple to show that in the  $\{|0_L\rangle, |1_L\rangle\}$  basis the exchange operators can be written as [6, 28]

$$\begin{aligned} E_{AB} &= E_{CD} = \begin{pmatrix} -1 & 0 \\ 0 & 1 \end{pmatrix} = -\bar{Z} \\ E_{AC} &= E_{BD} = \frac{\sqrt{3}}{2}\bar{X} + \frac{1}{2}\bar{Z} \\ E_{AD} &= E_{BC} = -\frac{\sqrt{3}}{2}\bar{X} + \frac{1}{2}\bar{Z}, \end{aligned} \quad (24)$$

where  $\bar{X}$ ,  $\bar{Z}$  are the encoded Pauli matrices  $\sigma_x$ ,  $\sigma_z$ , i.e. the Pauli matrices acting on the  $|0_L\rangle$ ,  $|1_L\rangle$  states. It follows from the Euler angle formula  $e^{-i\omega\mathbf{n}\cdot\boldsymbol{\sigma}} = e^{-i\beta\sigma_z}e^{-i\theta\sigma_x}e^{-i\alpha\sigma_z}$  (a rotation by angle  $\omega$  about the axis  $\mathbf{n}$ , given in terms of three successive rotations about the  $z$  and  $x$  axes) that one can perform all single encoded-qubit operations on the DFS states simply by switching the exchange interaction on and off. Note that the Euler angle formula is satisfied by any pair of non-parallel axes, although orthogonal axes may be more convenient. One can obtain an encoded  $\sigma_x$  operation by switching on two interactions simultaneously for the appropriate time intervals:

$$\bar{X} = -2(E_{AC} + \frac{1}{2}E_{AB})/\sqrt{3} = (E_{AC} - E_{AD})/\sqrt{3}.$$

Use of the Euler angle formula requires a Hamiltonian which is a sum of exchange terms with controllable coefficients  $J_{ij}(t)$ :

$$H_S = \sum_{i<j} J_{ij}(t)E_{ij}.$$

This is achievable, for example, by using local magnetic fields [1, 20, 21, 33, 34], by ferroelectric gates [35] or by optical rectification [36]. It is important to emphasize that the last two methods [35, 36] do not require magnetic field control, hence overcoming at least in part the problems with EQC raised in [22, 23]. This is an important advantage with regard to EQC, which renders these exclusively electrical control methods distinctly preferable to those using magnetic fields. However, residual magnetic fields, for example due to nuclear spin impurities, do remain a problem, especially in the group III–V semiconductors such as GaAs [37]. In silicon-based architectures this problem can be minimized by isotopic purification [38].

#### 4.2. Effect of the four-body terms on a single encoded qubit

Let us now consider how the four-body terms act on the DFS code. Using the results above, we find that

$$(\mathbf{S}_A \cdot \mathbf{S}_B)(\mathbf{S}_C \cdot \mathbf{S}_D) \simeq E_{AB}E_{CD} = (-\bar{Z})^2 = I$$

where  $I$  is the identity operator. Also,

$$\begin{aligned} E_{AC}E_{BD} &= \left( \frac{\sqrt{3}}{2}\bar{X} + \frac{1}{2}\bar{Z} \right)^2 \\ &= \frac{1}{4} \left[ 3I + I + \sqrt{3}(\bar{X}\bar{Z} + \bar{Z}\bar{X}) \right] = I \end{aligned}$$

and similarly  $E_{AD}E_{BC} = I$ . Thus all fourth-order terms  $(\mathbf{S}_i \cdot \mathbf{S}_j)(\mathbf{S}_k \cdot \mathbf{S}_l) \propto I$  as long we restrict their action to the subspace encoding one qubit. This implies that the encoding into the four-qubit DFS is immune to the fourth-order terms. In other words, when this encoding is used the problem of the computational errors induced by the undesired fourth-order terms simply disappears, as long as we restrict our attention to a single encoded qubit.

#### 4.3. Two encoded qubits

We must also be able to couple encoded qubits via a non-trivial gate such as controlled-phase:  $CP = \text{diag}(-1, 1, 1, 1)$ . This is one way to satisfy the requirements for universal quantum computation [39], though it is also possible to complete the set of single-qubit gates by measurements [40]. Two encoded qubits of the form (21), (22) occupy a four-dimensional subspace of the zero total spin subspace of eight spins. The zero total spin subspace is 14-dimensional. A very useful graphical way of seeing this, introduced in [6] but also known as a Bratteli diagram, is depicted in figure 9.

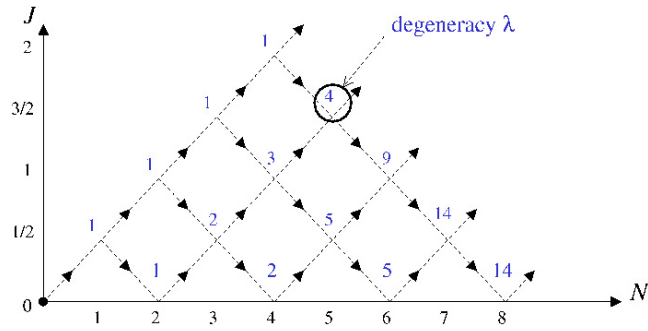


**Figure 9.** Partitioning of the Hilbert space of  $N$  spin-1/2 particles into DF subspaces (nodes of the graph). The integer above each node represents the number of paths leading from the origin to that node.

As more spins are added (horizontal axis) there are more possibilities for constructing a state with given total spin (vertical axis). In the case of four spins there are two paths leading from the origin to  $S_T = 0$ ; these correspond exactly to the  $|0_L\rangle$  and  $|1_L\rangle$  code states. For eight spins there are 14 such paths. Only four of these correspond to the four basis states  $\{|0_L0_L\rangle, |0_L1_L\rangle, |1_L0_L\rangle, |1_L1_L\rangle\}$ . It is convenient to label paths according to the intermediate total spin: the state  $|S_1, S_2, S_3, S_4, S_5, S_6, S_7, S_8\rangle$ , where  $S_k$  is the total spin of  $k$  spin-1/2 particles, uniquely corresponds to a path in figure 9 (we omit the origin in this notation) and the  $S_k$  form a complete set of commuting observables [6]. For example,

$$\begin{aligned}
 |0_L0_L\rangle &= |1/2, 0, 1/2, 0, 1/2, 0, 1/2, 0\rangle = \nearrow \searrow \nearrow \searrow \nearrow \searrow \nearrow \searrow \\
 |0_L1_L\rangle &= |1/2, 0, 1/2, 0, 1/2, 1, 1/2, 0\rangle = \nearrow \searrow \nearrow \searrow \nearrow \nearrow \searrow \searrow \\
 |1_L0_L\rangle &= |1/2, 1, 1/2, 0, 1/2, 0, 1/2, 0\rangle = \nearrow \nearrow \searrow \searrow \nearrow \searrow \nearrow \searrow \\
 |1_L1_L\rangle &= |1/2, 1, 1/2, 0, 1/2, 1, 1/2, 0\rangle = \nearrow \nearrow \searrow \searrow \nearrow \searrow \nearrow \searrow .
 \end{aligned}$$

On the right we have indicated the path in figure 9 corresponding to each state. The other 10 states with zero total spin can be similarly described. Thus the set of 14 states  $\{|S_1, S_2, S_3, S_4, S_5, S_6, S_7, 0\rangle\}$  forms a basis for the subspace of zero total spin of eight spin-1/2 particles. Henceforth we will find it convenient to represent exchange operators in this basis. We will order the 14 basis states as follows: first the four code states  $|0_L0_L\rangle, |0_L1_L\rangle, |1_L0_L\rangle, |1_L1_L\rangle$  as above, then

$$\begin{aligned}
 &|1/2, 0, 1/2, 1, 1/2, 0, 1/2, 0\rangle, |1/2, 1, 1/2, 1, 1/2, 0, 1/2, 0\rangle, \\
 &|1/2, 0, 1/2, 1, 1/2, 1, 1/2, 0\rangle, |1/2, 1, 1/2, 1, 1/2, 1, 1/2, 0\rangle, \\
 &|1/2, 0, 1/2, 1, 3/2, 1, 1/2, 0\rangle, |1/2, 1, 3/2, 1, 1/2, 0, 1/2, 0\rangle, \\
 &|1/2, 1, 3/2, 1, 3/2, 1, 1/2, 0\rangle, |1/2, 1, 3/2, 2, 3/2, 1, 1/2, 0\rangle, \\
 &|1/2, 1, 1/2, 1, 3/2, 1, 1/2, 0\rangle, |1/2, 1, 3/2, 1, 1/2, 1, 1/2, 0\rangle.
 \end{aligned}$$



where

$$U_A = \exp \left[ -\frac{i}{2} \cos^{-1}(-1/3) E_{DE} \right]$$

$$U_B = \exp \left[ -\frac{i\pi}{2} \sum_{A=i < j}^D E_{ij} \right].$$

In terms of these gates the controlled-phase gate can be written as

$$CP = U_1^\dagger (U_2^\dagger U_3^\dagger) U_5^\dagger U_6 U_5 (U_3 U_2) U_1, \tag{25}$$

where  $U_3 U_2$  can be executed in one step since by inspection the two gates operate on the two blocks separately (and identically). This gate sequence operates in the entire 14-dimensional subspace of  $S_T = 0$  states of eight spins: the code space is left after application of  $U_1$ , but is returned to at the end of the sequence when  $U_1^\dagger$  is applied. Hence our single-qubit considerations above do not apply: even if a four-body interaction acts as the identity operator on a single encoded qubit, it may act non-trivially in the larger  $S_T = 0$  space. We must therefore carefully analyse the action of this gate sequence in light of the three- and four-body corrections.

The key point in Bacon’s construction of the gate sequence is to ensure that each gate acts ‘classically’, i.e. it only couples a given  $S_T = 0$  basis state to another without creating superpositions of such basis states (that the gates above act in this manner is not at all simple to see directly, but is the reason for the particular choice of angles in the gates). We find that, in order to still satisfy this key criterion, it is necessary to tune the four-body exchange coupling constants. Thus to enact a  $CP$  gate in the presence of four-body interactions, there needs to be sufficient flexibility in tuning the four-body coupling. We note that there are other ways to obtain a  $CP$  gate [31]; our present goal is mainly to explore the implications of the four-body terms in a context of some general interest.

A detailed matrix calculation (see the appendix) shows us that the effect of nearly every gate in (25) depends upon the relative strengths of the exchange coefficients between the various pairs or quartets of dots it couples, as in

$$CP' = U_1^\dagger (J'_a, J'_b, J'_c, J'_d) \left[ U_2^\dagger (J'_2, J''_2) U_3^\dagger (J'_3, J''_3) \right] U_5^\dagger U'_6 (J'_B) U'_5$$

$$\times \left[ U'_3 (J'_3, J''_3) U'_2 (J'_2, J''_2) \right] U_1 (J'_a, J'_b, J'_c, J'_d)$$

where the parameters  $\{J\}$  are determined by the shapes and strengths of the individual dot confining potentials. Comparison with the results of [30] then yields the following relations between these new coefficients:

- (1) The constant  $J'_c$  can take on an arbitrary value.
- (2) The constants  $J'_2$  and  $J''_2$  must be chosen to satisfy the transcendental equation  $\eta = 0$  (see the appendix).
- (3) The constants  $J'_3$  and  $J''_3$  must be chosen to satisfy the transcendental equation  $\eta = 0$  (see the appendix).
- (4) The constant  $J'_5$  must either be zero or chosen such that  $\sqrt{\frac{4}{3}(J'_5)^2 - 2J'_5 + 1}$  is an even integer.
- (5) The constant  $J'_B$  must be an integer.
- (6) The constants  $J'_a, J'_b, J'_d$  can take on an infinite set of rationally related values, wherein the ratio of any pair (e.g.,  $J'_b/J'_d$ ) can be chosen completely arbitrarily and the value of the third constant is determined by this choice.

The most restrictive of these conditions is that  $J'_B$  must be an integer. However, note that since the gates are applied sequentially this condition need only be satisfied during the application of the  $U'_6$  gate, and it is plausible from the earlier sections of this paper that corresponding Heisenberg exchange constants can be found. When these conditions are satisfied it is indeed the case that  $CP' = (-1, 1, 1, 1)$  on the code space.

#### 4.5. Dimensionality of parameter spaces required by two-body and four-body couplings

We caution that, although the encoding procedure described above has been shown mathematically to remove the effect of the four-body couplings, the experimental construction of a suitable apparatus using real quantum dots is another matter, as the following heuristic calculation suggests.

Our modified gates imply the following constraints on the coupling coefficients (see the appendix for the definitions of  $\Lambda$  and  $\eta$ ):

$U'_5$  gate

- (a)  $K_2[FG] = \frac{1}{2}K_2[GH]$ ;
- (b) Either  $K_2[FH] = 0$  or  $\Lambda(K_2[FH]) = 2n$ , where  $n$  must have an integer value;

$U'_B$  gate

- (c)  $K_2[ij]$  is the same for all pairs within  $\{A, B, C, D\}$ ;
- (d)  $K_4[ABCD] = K_4[ACBD] = K_4[ADBC]$ ;
- (e)  $K_4[ABCD] = 2mK_2[AB]$ , where  $m$  may have any integer value;

$U'_2$  gate

- (f)  $K_2[FG] = K_2[FH] = K_2[GH]$ ;
- (g)  $K_2[EF] = \frac{9}{2}K_2[GH]$ ;
- (h)  $K_4[EGFH] = K_4[EHFG]$ ;
- (i) Either  $K_4[EFGH] = K_4[EGFH]$ , or  $K_4[EFGH]$  and  $K_4[EGFH]$  satisfy the transcendental equation  $\eta(K_4[EFGH], K_4[EGFH]) = 0$ ;

$U'_3$  gate

- (j)  $K_2[AB] = K_2[AC] = K_2[BC]$ ;
- (k)  $K_2[CD] = \frac{9}{2}K_2[AB]$ ;
- (l)  $K_4[ACBD] = K_4[ADBC]$ ;
- (m) Either  $K_4[ABCD] = K_4[ACBD]$ , or  $K_4[ABCD]$  and  $K_4[ACBD]$  satisfy the transcendental equation  $\eta(K_4[ABCD], K_4[ACBD]) = 0$ ;

$U'_1$  gate

- (n)  $K_2[ij]$  is the same for all pairs within  $\{A, B, C, D\}$ ;
- (o)  $K_2[DE] = 2K_2[AB]$ ;
- (p)  $K_4[ABCD] = K_4[ACBD] = K_4[ADBC]$ ;
- (q)  $K_4[ABCE] = K_4[ACBE] = K_4[AEBCE]$ ;
- (r)  $K_4[ADBE] = K_4[AEBD]$ ;
- (s)  $K_4[ADCE] = K_4[AECD]$ ;
- (t)  $K_4[BDCE] = K_4[BECD]$ ;
- (u)  $K_4[ADBE] = K_4[ADCE] = K_4[BDCE]$ ;
- (v)  $K_4[ABDE]$  is a certain single-valued function of  $K_4[ADBE]$ ;
- (w)  $K_4[BCDE]$  is a certain single-valued function of  $K_4[ADCE]$ ;
- (x)  $K_4[ACDE]$  is a certain single-valued function of  $K_4[BDCE]$ .



Since the coupling coefficients must in general vary with time in order to satisfy all of these constraints (for example,  $K_2[CD]$  and  $K_2[AC]$  would be equal during the operation of  $U'_B$  but unequal during  $U'_3$ ), we also assume that particular constraints need to be concurrently satisfied only when they arise from the same gate.

We first note that, by the same reasoning used to derive (6) and (18), a four-dot Hamiltonian for the geometry of  $\{A, B, C, E\}$  contains a constant term and nine independent coupling coefficients. If these nine coefficients assumed a given set of values and we wished to adjust them to meet constraints such as those listed above, we would need nine additional degrees of freedom in the system. We make the conservative assumption, however, that one two-body coefficient and one four-body coefficient can be left unaltered and the others adjusted to correspond to them, which means that only seven additional parameters are required. Similarly, for the subset  $\{A, B, D, E\}$  ( $\{A, C, D, E\}$ ,  $\{B, C, D, E\}$ ,  $\{A, B, C, D\}$ ), there are 9 (6, 7, 5) independent coupling coefficients for which we require 7 (4, 5, 3) tunable parameters if a given set of constraints are to be satisfied. We will of course count one more degree of freedom when a constraint includes relationships between the two-body and four-body energies.

Now suppose that we designate one 'base' choice of  $\{x_b, x_c, x_v\}$  such that, within each of the two squares, all the quantities  $K_2[ij]$  are equal, all the quantities  $K_4[ijkl]$  are equal and  $K_4[ijkl] = 2K_2[ij]$ . That arrangement can simultaneously satisfy constraints (b), (c), (d), (e), (f), (h), (i), (j), (l), (m), (n) and (p) provided that the value of  $K_2[FH]$  is chosen appropriately. From this potential, we would need to make one change within  $\{E, F, G, H\}$  to reach condition (a) or condition (g), or one change within  $\{5, 6, 7, 8\}$  to obtain (k) or (o). The couplings of  $\{A, B, C, E\}$  must be adjusted to match (q) while still satisfying (n), (o) and (p) which requires six additional degrees of freedom as explained in the preceding paragraph. Similarly, (v) ((w), (x)) and (r) ((s), (t)) together imply particular adjustments to the four-body couplings in  $\{A, B, D, E\}$  ( $\{A, C, D, E\}$ ,  $\{B, C, D, E\}$ ) which require 6 (3,4) new parameters. (The single-valued function in question is the same for all three cases, so  $K_4[ABDE]$  ends up equalling  $K_4[ACDE]$  and  $K_4[BCDE]$ .) Finally, we need two more degrees of freedom available somewhere in order to meet constraint (u), for a grand total of 28 degrees of freedom.

To put the size of this number into perspective we also count the independently tuned energies necessary to meet the conditions on EQC using pairwise couplings alone. By choosing a suitable combination  $\{x_b, x_c, x_v\}$  for an entire eight-spin system, we could satisfy (b), (c), (f), (j) and (n) at the same time; one more degree of freedom would be necessary to also satisfy (o). Starting from such a system we could presumably satisfy (a) or (g) by adjusting one parameter within  $\{E, F, G, H\}$ , or satisfy (k) by adjusting one parameter within  $\{A, B, C, D\}$ . Hence we estimate that seven degrees of freedom are required for the purely Heisenberg Hamiltonian considered in [30]. We see that, even if one presupposes the ability to create and position many identical qubits of the form (21), (22) (three free parameters), accounting correctly for two-body and four-body coupling is still a great deal more demanding than two-body coupling alone. It is this experimental challenge that must be weighed against the increased length (and hence vulnerability to decoherence) of pulse sequences employing only two-body couplings [31].

## 5. Summary and conclusions

Earlier work [17, 18] showed that in highly symmetrical geometries the interaction between three and four mutually interacting electrons confined in parabolic potentials contains many-body terms, which in the case of four electrons qualitatively modify the usual Heisenberg interaction. In this work we have improved upon these early results by considering realistic linear and square geometries and by utilizing Gaussian confining potentials. Specifically, we have shown in a Heitler–London calculation that in the case of four mutually interacting













- [3] Preskill J 1998 *Proc. R. Soc. A* **454** 385
- [4] Raussendorf R and Briegel H J 2001 *Phys. Rev. Lett.* **86** 5188
- [5] Bacon D, Kempe J, Lidar D A and Whaley K B 2000 *Phys. Rev. Lett.* **85** 1758
- [6] Kempe J, Bacon D, Lidar D A and Whaley K B 2003 *Phys. Rev. A* **63** 042307
- [7] DiVincenzo D P, Bacon D, Kempe J, Burkard G and Whaley K B 2000 *Nature* **408** 339
- [8] Bacon D, Kempe J, DiVincenzo D P, Lidar D A and Whaley K B 2001 Encoded universality in physical implementations of quantum computers *Proc. 1st Int. Conf. on Experimental Implementations of Quantum Computation (Sydney)* ed R Clark (Princeton, NJ: Rinton) p 257
- [9] Lidar D A and Wu L-A 2002 *Phys. Rev. Lett.* **88** 017905
- [10] Bacon D, Brown K R and Whaley K B 2001 *Phys. Rev. Lett.* **87** 247902
- [11] Farhi E, Goldstone J, Gutmann S, Lapan J, Lundgren A and Preda D 2001 *Science* **292** 472
- [12] Shor P W 1996 Fault-tolerant quantum computation *Proc. 37th Symp. Foundations of Computing* (Los Alamitos, CA: IEEE Computer Society Press) p 56
- [13] Gottesman D 1997 *Phys. Rev. A* **57** 127
- [14] Steane A M 1999 *Nature* **399** 124
- [15] Lidar D A, Bacon D, Kempe J and Whaley K B 2001 *Phys. Rev. A* **63** 022307
- [16] Freedman M H 2003 *Commun. Math. Phys.* **234** 129
- [17] Mizel A and Lidar D A 2004 *Phys. Rev. Lett.* **92** 077903
- [18] Mizel A and Lidar D A 2004 *Phys. Rev. B* **70** 115310
- [19] Waugh F R, Berry M J, Crouch C H, Livermore C, Mar D J, Westervelt R M, Campman K L and Gossard A C 1996 *Phys. Rev. B* **53** 1413
- [20] Burkard G, Engel H-A and Loss D 2000 *Fortschr. Phys.* **48** 965
- [21] Hu X and Das Sarma S 2000 *Phys. Rev. A* **61** 062301
- [22] Scarola V W, Park K and Das Sarma S 2004 *Phys. Rev. Lett.* **93** 120503
- [23] Scarola V W and Das Sarma S 2005 *Phys. Rev. A* **71** 032340
- [24] Zanardi P 1999 *Phys. Rev. A* **60** R729
- [25] Wu L-A and Lidar D A 2002 *Phys. Rev. Lett.* **88** 207902
- [26] Wu L-A, Byrd M S and Lidar D A 2002 *Phys. Rev. Lett.* **89** 127901
- [27] Zanardi P and Rasetti M 1997 *Phys. Rev. Lett.* **79** 3306
- [28] Lidar D A, Bacon D, Kempe J and Whaley K B 2000 *Phys. Rev. A* **61** 052307
- [29] Lidar D A and Whaley K B 2003 Decoherence-free subspaces and subsystems *Irreversible Quantum Dynamics (Springer Lecture Notes in Physics vol 622)* (Berlin: Springer) p 83
- [30] Bacon D M 2001 Decoherence, control and symmetry in quantum computers *Preprint quant-ph/0305025*
- [31] Hsieh M, Kempe J, Myrgren S and Whaley K B 2004 *Quantum Inf. Process.* **2** 289
- [32] Heitler W and London F 1927 *Z. Phys.* **44** 455
- [33] Burkard G, Loss D and DiVincenzo D P 1999 *Phys. Rev. B* **59** 2070
- [34] Hu X and Das Sarma S 2001 *Phys. Rev. A* **64** 042312
- [35] Levy J 2002 *Phys. Rev. Lett.* **89** 147902
- [36] Levy J 2002 *Phys. Status Solidi b* **233** 467
- [37] de Sousa R and Das Sarma S 2003 *Phys. Rev. B* **68** 115322
- [38] Yablonovitch E, Jiang H W, Kosaka H, Robinson H D, Rao D S and Szkopek T 2003 *Proc. IEEE* **91** 761
- [39] Barenco A, Bennett C H, Cleve R, DiVincenzo D P, Margolus N, Shor P, Sleator T, Smolin J and Weinfurter H 1995 *Phys. Rev. A* **52** 3457
- [40] Knill E, Laflamme R and Milburn G J 2001 *Nature* **409** 46